FLUID DYNAMIC FORCES IN THE MAIN STEAM PIPELINE OF THERMAL POWER PLANT UPON STOP VALVES CLOSURE

by

Vladimir D. STEVANOVIĆ*, Sanja S. MILIVOJEVIĆ, and Milan M. PETROVIĆ
Faculty of Mechanical Engineering, University of Belgrade, Belgrade, Serbia

Original scientific paper
https://doi.org/10.2298/TSCI190915426S

A steam turbine trip is followed by a prompt closure of stop valves in front of the turbine and consequently to a pressure rise in the main steam pipeline. This steam hammer transient leads to the generation of intensive fluid dynamic forces that act along the pipeline axis and induce additional dynamic loads on the main steam pipeline. It is a common practice to assume a simultaneous closure of all stop valves in the safety analysis of the main steam pipeline. In the present paper computer simulations and analyses of the fluid dynamic forces are performed for several scenarios that take into account the possibility of delayed closure of the stop valve in front of the turbine. The influence of the failure of the steam by-pass line opening is considered too. The results show that the delay of the stop valve closure increases the maximum intensity of fluid dynamic force in the pipeline segment in front of the stop valve and decreases the intensity of fluid dynamic forces in segments along the pipeline. The failure of the by-pass line to open leads to prolonged steam pressure and fluid dynamic forces oscillation in pipeline segments. The simulations were performed with the in-house computer code based on the method of characteristics for the solving of the hyperbolic system of PDE that represent the mass, momentum and energy balance equations of the 1-D, compressible and transient fluid-flow. The obtained results are a support to safety analyses of thermal power plants under transient conditions.

Key words: *static and dynamic loads, calculation methodology, safety analysis*

Introduction

The main steam pipeline in the thermal power plant conveys steam at high pressure and temperature from the steam boiler to the high pressure turbine (HPT). It is a vital plant system and its integrity is extremely important for the safety of thermal power plant. The main steam pipeline is subjected to maximum dynamic loads during a turbine trip, which is followed by an instantaneous closure of the stop valves in front of the HPT and opening of the steam by-pass line. The valves closure leads to the pressure increase in the steam pipeline, which is also characterized as the steam hammer. This propagation of pressure waves along the pipeline leads to the generation of the fluid dynamic forces that act along the pipe axis [1]. The prediction of the fluid dynamic forces is crucial for the stress and strain analyses and design of structure, supports and hangers of the pipeline [2]. The prediction of the fluid dynamic forces in the pipeline systems is a necessary part of the thermal power plant safety analyses [3].

* Corresponding author, e-mail: vstevanovic@mas.bg.ac.rs

A few examples of the steam hammer transients that occurred in the operating power plants and are important for the plant safety are reported here. Excess dynamic loads of the steam pipeline systems were experienced in the nuclear power plants during transients of stop valves closure and opening of relief valves [4]. The fluid dynamic forces in the main steam pipeline during the turbine trip and a subsequent pipe break in front of the stop valve was reported in [5]. An analysis of the steam hammer event in the hot reheat line of the thermal power plant was presented in [6].

A reliable approach to the numerical simulation of the pressure transients in the pipeline networks is based on the application of the method of characteristics for the solving of mass, momentum and energy balance equations of 1-D, transient and compressible fluid-flow [7]. As stated in [7] *the Method of Characteristic is the only method which tracks accurately the propagation of discontinuities in the first-order derivatives; the characteristic co-ordinates are Lagrangian co-ordinates for such discontinuities.* In addition, the method of characteristics allows an accurate modelling of all types of boundary conditions that can be encountered in the complex pipeline networks and lines. This method was applied in a number of numerical investigations of pipeline transients, such as in simulation and analyses that are mentioned in the previous paragraph [4-6], as well as in some established computer codes: CHARME-01 [8], PIPES [9], PIPENET VISION [10], to mention a few.

Previous analyses of the steam hammer transient in the main steam pipeline of thermal power plants were performed with the simultaneous closure of all stop valves in front of the HPT [4-6]. There is a possibility for a delayed closure of the stop valve. In the present paper the influence of the delayed closure of the stop valve on the intensity of fluid dynamic forces is investigated during the HPT trip transient in 350 MWe coal-fired thermal power plant. The failure of the steam by-pass line from the main steam pipeline towards the steam reheat line is also taken into account. The numerical simulations were performed with the in-house code based on the method of characteristics. The code was developed at the Faculty of Mechanical Engineering at the University of Belgrade. The results obtained with the failure and regular opening of the by-pass line, as well as with the simultaneous and delayed closure of stop valve are compared. The influence of these scenarios on the intensity of fluid dynamic forces is discussed and recommendations for the safety analyses are underlined.

Calculation methodology

Transient flow of compressible homogeneous fluid is described by 1-D model, based on non-stationary mass, momentum and energy balance equations:

– Mass conservation:

$$\frac{\mathrm{D}\rho}{\mathrm{D}t} + \rho\frac{\partial u}{\partial z} = 0 \tag{1}$$

– Momentum conservation:

$$\frac{\mathrm{D}u}{\mathrm{D}t} + \frac{1}{\rho}\frac{\partial p}{\partial z} + \frac{fu|u|}{2d} + \mathrm{g}\sin\theta = 0 \tag{2}$$

– Energy conservation:

$$\frac{\mathrm{D}h}{\mathrm{D}t} - \frac{1}{\rho}\frac{\mathrm{D}p}{\mathrm{D}t} - \frac{fu|u|^2}{2d} - \frac{\dot{q}}{\rho} = 0 \tag{3}$$

where the material derivative is D/Dt = $\partial/\partial t + u\partial/\partial z$, the dependent variables are velocity, u [ms^{-1}], pressure, p [Pa], and fluid enthalpy, h [Jkg^{-1}], and the independent variables are time, t [s], and spatial co-ordinate, z [m]. The third term on the left-hand side of eqs. (2) and (3) is related to the fluid friction on the pipe's wall, where f [–] denotes Darcy friction factor, d [m] – the hydraulic diameter of the pipe, θ [°] – the angle of pipe inclination, and g [ms^{-2}] – the gravity constant. The fourth term in eq. (3) represents heat flow rate exchanged per unit mass of fluid. The additional equation is equation of state in the form of density dependence on pressure and enthalpy $\rho = \rho(p,h)$ [kgm^{-3}]. The flow channel area A [m^2] is constant. The pipe wall is assumed to be rigid, which is appropriate in case of the main steam pipeline thick walls.

The obtained system of hyperbolic PDE is solved by the method of characteristics for appropriate initial and boundary conditions. The method of characteristics has high accuracy since it reduces hyperbolic partial differential equations to ODE and it has ability to accurately track pressure wave and enthalpy front propagations [7]. The transformation of eqs. (1)-(3) into ODE is performed along three characteristic paths in the space and time co-ordinate system, as presented in fig. 1. Characteristic paths C^+ and C^- correspond to the pressure wave propagation and to enthalpy front propagation. The following set of the ODE is derived from the balance eqs. (1)-(3):

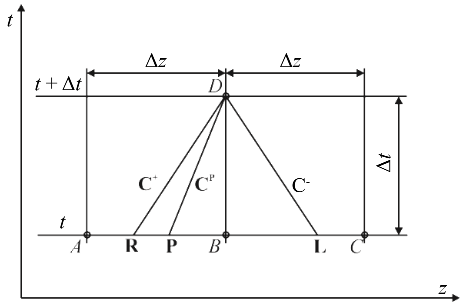

Figure 1. Space-time co-ordinate system and characteristic paths

$$\mathrm{d}p + \rho c \mathrm{d}u = (X + \rho c Y)\mathrm{d}t \quad \text{for the characteristic path C+ that reads } \frac{\mathrm{d}t}{\mathrm{d}x} = \frac{1}{u+c} \tag{4}$$

$$\mathrm{d}p - \rho c \mathrm{d}u = (X - \rho c Y)\mathrm{d}t \quad \text{for the characteristic path C}^- \text{ that reads } \frac{\mathrm{d}t}{\mathrm{d}x} = \frac{1}{u-c} \tag{5}$$

$$\mathrm{d}h - \frac{\mathrm{d}p}{\rho} = Z\mathrm{d}t \quad \text{for the characteristic path C}^\mathrm{P} \text{ that reads } \frac{\mathrm{d}t}{\mathrm{d}x} = \frac{1}{u} \tag{6}$$

where

$$X = -c^2 \left(\frac{\partial \rho}{\partial h}\right)_p \left(\frac{fu^2|u|}{2d} - \mathrm{g}u\sin\theta + \frac{\dot{q}}{\rho}\right) \tag{7}$$

$$Y = -\frac{fu|u|}{2d} - \mathrm{g}\sin\theta \tag{8}$$

$$Z = \frac{fu^2|u|}{2d} - \mathrm{g}u\sin\theta + \frac{\dot{q}}{\rho} \tag{9}$$

The total differentials in the eqs. (4)-(6) are approximated with finite differences along the corresponding characteristics paths C^+, C^-, and C^P that are presented in fig. 1, and the following set of algebraic equations is obtained:

$$(p_D - p_R) + \rho_R c_R (u_D - u_R) = \left(X_R + \rho_R c_R Y_R\right)\Delta t \quad \text{for} \quad \frac{\Delta t}{\Delta x} = \frac{1}{u_R + c_R} \tag{10}$$

$$(p_D - p_L) - \rho_L c_L (u_D - u_L) = \left(X_L - \rho_L c_L Y_L\right)\Delta t \quad \text{for} \quad \frac{\Delta t}{\Delta x} = \frac{1}{u_L - c_L} \tag{11}$$

$$(h_D - h_P) - \frac{(p_D - p_P)}{\rho_P} = Z_P \Delta t \quad \text{for} \quad \frac{\Delta t}{\Delta x} = \frac{1}{u_P} \tag{12}$$

Explicit expressions are derived from eqs. (10)-(12) for the calculation of the dependant parameters u_D, p_D, and h_D in the point D at the new time $t+\Delta t$, fig. 1. Velocity, pressure and enthalpy values in points R, L, and P are calculated by linear interpolations between known pair of values in nodes A and B, as well as in B and C at the initial time t, fig. 1.

The time step of integration, denoted with Δt [s], is determined according to the Courant criterion:

$$\Delta t \le \min\left(\frac{\Delta z}{c_i + |u_i|}\right), \quad i = 1, 2, ...N \tag{13}$$

where c [ms^{-1}] is the speed of sound, N – the number of nodes in all pipes and the index i denotes nodes along pipes. The spatial step of integration, Δz [m] in eq. (13), is the distance between adjacent nodes and it is constant for the whole pipeline.

Boundary conditions are defined in order to calculate the flow parameters at the junction of two or more pipes within the pipeline network, as well as the steam inlets to the pipeline from the boiler headers and outlets at the stop valves in front of the turbines and at the valve in the steam by-pass line. Additional equations (mass, momentum and energy balances) must be added for the ends of a pipeline. These equations are substitution for the equation of characteristics which does not belong to a physical domain of the pipe. General form of these additional boundary conditions is presented as follows:

– Mass balance at the boundary:

$$\Delta(\rho u A) = 0 \tag{14}$$

– Momentum balance at the boundary:

$$\Delta\left(\frac{\rho u^2}{2}\right) + \Delta p = \Delta M(t) \tag{15}$$

– Energy balance at the boundary:

$$\Delta\left(h + \frac{u^2}{2}\right) = 0 \tag{16}$$

where $\Delta M(t)$ is the momentum loss at the valves or junctions.

The fluid dynamic force, which intensity is denoted as F [N], acts along the pipe axis. It is a direct consequence of the mass-flow rate $\dot{m}$ [kgs^{-1}] change [1]:

$$F = \int_L \frac{\mathrm{d}\dot{m}}{\mathrm{d}t}\mathrm{d}z \tag{17}$$

The fluid dynamic force has an impact character and causes an additional load to pipe structure, supports and hangers. The positive value of the fluid dynamic force corresponds to the direction of the flow before disturbance.

The described model is implemented in the in-house code. The solving algorithm is presented in fig. 2. The code was validated for several transient conditions, such as: the main steam pipeline break [5], water hammers in two-phase systems [11], water hammer with gaseous cavitation [12] and natural gas pipeline transients [13].

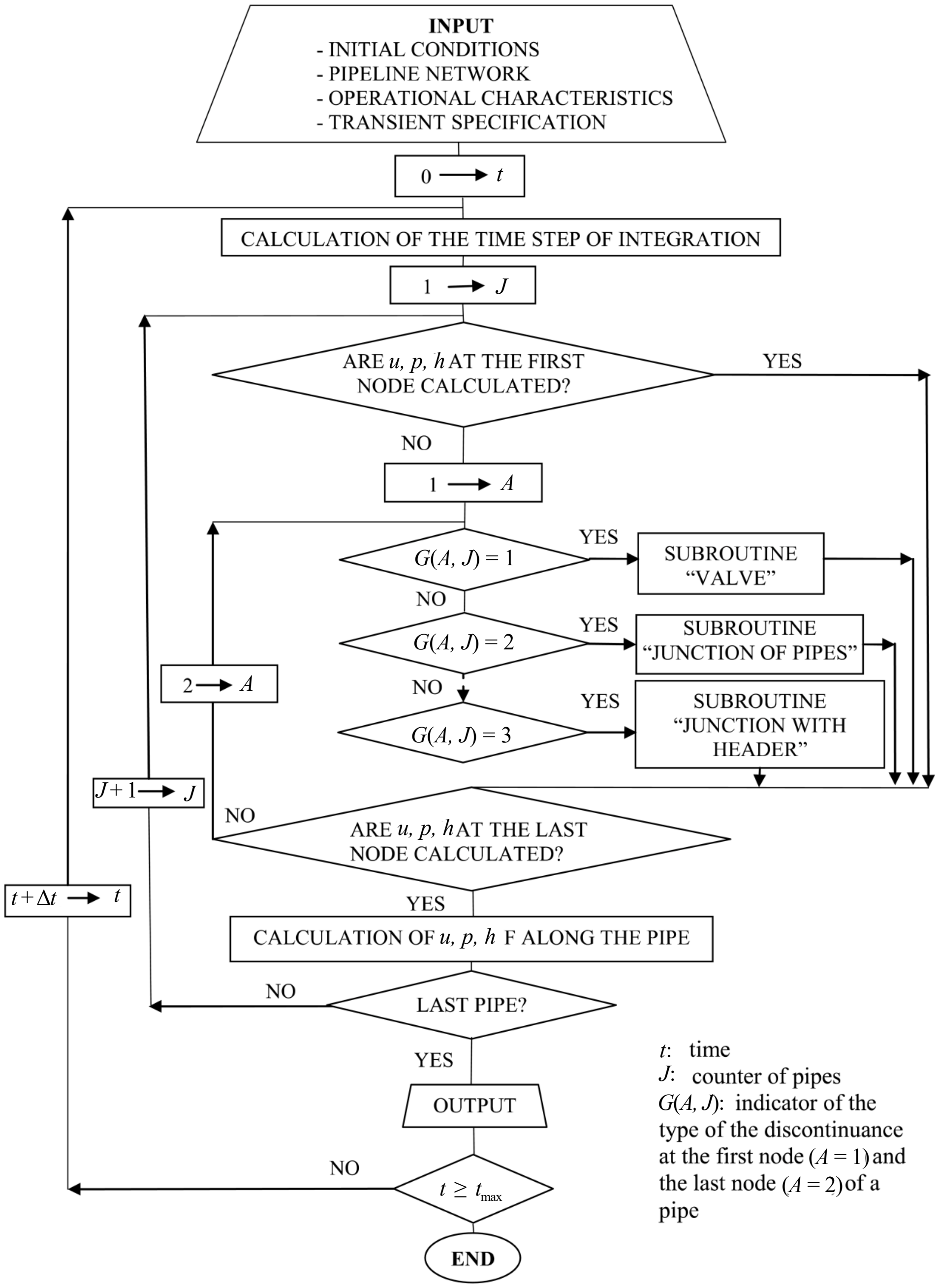

Figure 2. Flowchart of the calculation procedure

Main steam pipeline in the thermal power plant

The isometric view of the main steam pipeline in 350 MWe thermal power plant is shown in fig. 3. The steam pipeline is supplied with fresh steam from the outlet headers of the steam boiler

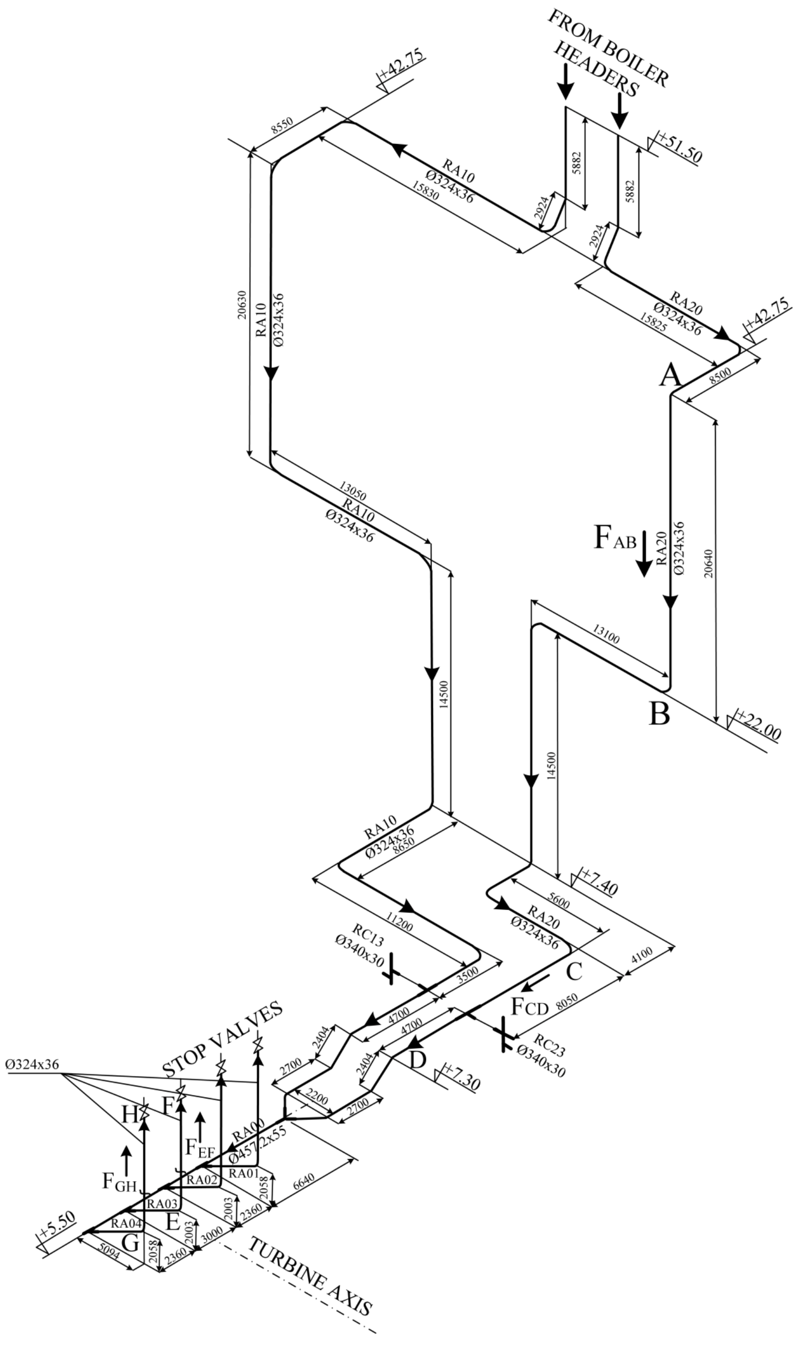

Figure 3. Isometric view of the main steam pipeline

superheater at the temperature of 540 °C and pressure of 186 bar. Steam flows through two branches RA 10 and RA 20, which are connected with the wye junction into the main collector of the fresh steam RA 00. The RA 10 branch is about 5% longer than the RA 20 branch, which leads to about 2.3% greater mass-flow rate in RA 20 branch. This relation is derived under the assumption that the pressure values at the inlet of RA 10 and RA 20 branches are the same, *i.e.* the pressure drops from the RA 10 and RA 20 inlets to the mutual wye junction are the same. Further, according to the Darcy equation for pressure drop calculation, the following relation holds $(\dot{m}_{\mathrm{RA}20}/\dot{m}_{\mathrm{RA}10})^2 = l_{\mathrm{RA}10}/l_{\mathrm{RA}20}$. This small difference in the mass-flow rates through RA 10 and RA20 branches is taken into account. The high pressure by-pass lines RC 13 and RC 23 are connected, respectively, to the horizontal sections of branches RA 10 and RA 20 in front of the wye junction. Valves in the by-pass lines open in case of the turbine trip and convey steam to the cold reheat steam line RC, from which the steam is further transported to the turbine condenser. Steam flows to the HPT from the collector RA 00 through four admission lines RA 01, RA 02, RA 03, and RA 04. The admission lines are connected to the collector by T junctions. All four lines RA 01, RA 02, RA 03, and RA 04 are equipped with the stop control valves in front of the HPT. The initial pressure and temperature of fresh steam in front of the stop valves are 179 bar and 537 °C.

Numerical simulation of the main steam pipeline transient during turbine trip

In order to determine the maximum dynamic forces generated in the main steam pipeline, the numerical simulations were made for the following three scenarios:

- Simultaneous closure of all four stop valves in 0.15 seconds in front of the HPT with closed valves on the steam by-pass lines around the HPT,
- Simultaneous closure of all four stop valves in 0.15 seconds in front of the HPT with opening of the valves on the steam by-pass lines around the HPT in 0.2 seconds,
- Four scenarios with simultaneous closure of three stop valves in front of the HPT in 0.15 seconds and with delayed closure of the fourth valve by 0.5 seconds (the valves on the by-pass lines around the HPT remain closed).

Likelihood of the above listed scenarios with closed by-pass lines during the turbine trip and with delayed closing of one valve cannot be excluded. Therefore, they are taken into account in order to determine the maximum values of fluid dynamic forces that could be generated within the main steam pipeline RA.

The main steam pipeline system presented in section *Main steam pipeline in the thermal power plant* is discretized for the numerical simulations with nodes determined with the constant length between two adjacent nodes of $\Delta z = 0.3$ m. Further reduction of the spatial step Δz has no influence on the obtained results. The main steam pipeline is thermally insulated. Regarding this fact and due to the short time periods of few seconds of the simulated transients, it is assumed that the main steam pipeline is adiabatically insulated. Hence, the heat source term $\dot{q}$ in the energy balance eq. (3) is equal to zero.

Figures 4-9 show dynamic forces and pressure in sections of the RA steam pipeline that are calculated according to first and second scenarios. All four stop valves simultaneously close and by-pass lines remain closed, first scenario or valves on the by-pass lines open, second scenario. Labels of the pipeline sections that are referred in the figure captions are shown in fig. 3. The dynamic forces in figs. 4-6 are determined for the following straight sections of the steam pipeline: the section G-H directly in front of the stop valve 4.6 m long, fig. 4, the section C-D containing the T-junction by which it is connected to the by-pass line, 12.7 m long, fig. 5, and a vertical section A-B at the boiler outlet, 20.64 m long, fig. 6. The results show that the maximum

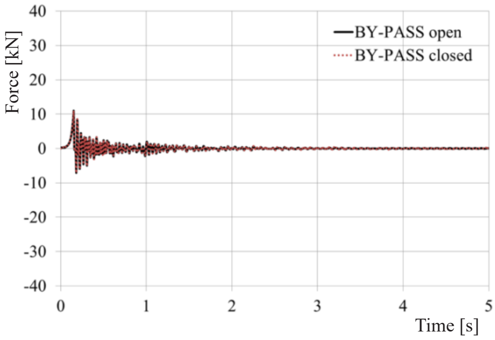

Figure 4. Dynamic force F_{GH} in the RA 04 section in front of the stop valve, in cases with simultaneous closing of all stop valves and with and without opening of the by-pass lines
(*for color image see journal web site*)

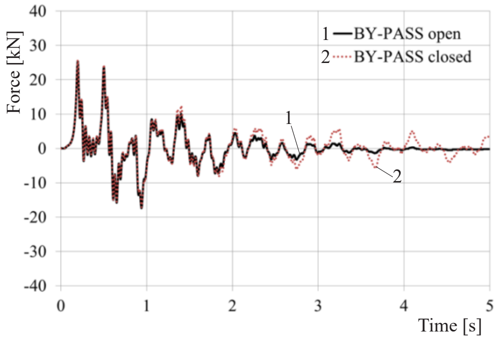

Figure 5. Dynamic force F_{CD} in the RA 20 section, in cases with simultaneous closing of all stop valves and with and without opening of the by-pass lines
(*for color image see journal web site*)

amplitudes of the dynamic forces occur within a period of up to one second after the stop valve closure and that they attenuate over the next few seconds. The amplitudes of the forces increase with the length of the straight section of the pipeline, which is the result of the integration of the mass-flow rate change with time along the section length, as presented with eq. (17). In the section 4.6 m long just in front of the stop valve, the maximum force amplitude is approximately 11 kN, fig. 4, in the section 12.7 m long maximum force amplitude is approximately 26 kN, fig. 5, while in the longest section of 20.64 m it reaches a value of approximately 37 kN, fig. 6. A positive value of the force means that the force acts in the original direction of steam flow, from the boiler to the turbine, while a negative value indicates the opposite direction of the force action. The dynamic force values are practically the same in the section directly in front of the stop valves for both scenarios, with open and closed by-pass lines. In other sections, the dynamic forces in cases of open and closed by-pass lines are practically the same for the first second, while after that the attenuation of the dynamic forces is greater in case with the opened by-pass valves. Figures 7-9 show periodic pressure changes in the RA line, which occur due to the periodic propagation of pressure waves between the closed stop valves and the outlet headers of the steam boiler. A maximum pressure amplitude of approximately 25 bar is reached in front

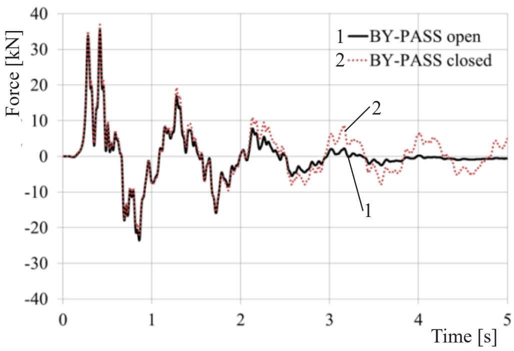

Figure 6. Dynamic force F_{AB} in the RA 20 section, in cases with simultaneous closing of all stop valves and with and without opening of the by-pass lines

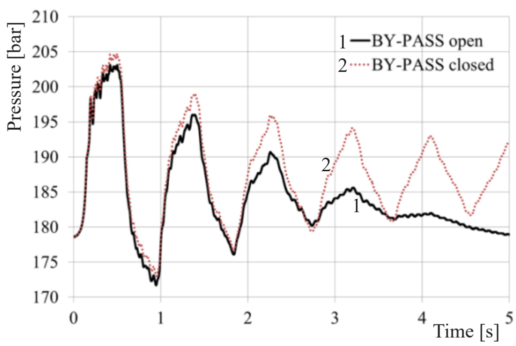

Figure 7. Steam pressure in the RA 04 section in front of the stop valve, in cases with simultaneous closing of all stop valves and with and without opening of the by-pass lines

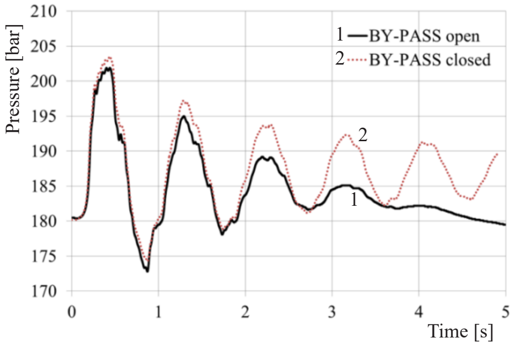

Figure 8. Steam pressure at the junction of the RA 20 and RC 23 sections, in cases with simultaneous closing of all stop valves and with and without opening of the by-pass lines

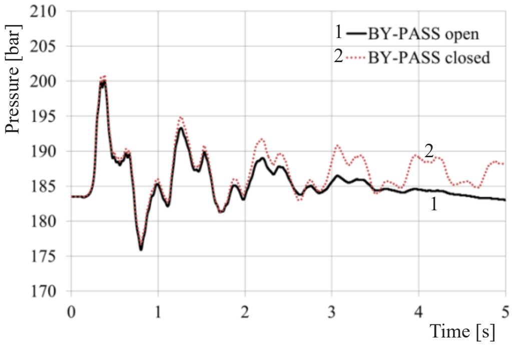

Figure 9. Steam pressure at the half length of the A-B part of the RA 20 section, in cases with simultaneous closing of all stop valves and with and without opening of the by-pass lines

of the stop valve immediately after its closure in case with the by-pass line opening, while this amplitude is about 2 bar higher in case with the closed by-pass line, fig. 7. The amplitude of the first pressure peak is reduced from the stop valve towards the boiler. Figure 8 shows that the first pressure amplitude is about 22 bar at the junction of the RA 20 line with the by-pass line RC 23, in case with the by-pass line opening, while the amplitude is about 1 bar higher in case with the closed by-pass line. Figure 9 shows that the first pressure amplitude is about 17 bar in case with the opening of the by-pass line, while this amplitude is negligibly higher in case with the closed by-pass line. As shown in figs. 7-9, the pressure amplitudes are attenuated in the course of time. In case with a closed by-pass line, the pressure oscillates with attenuating amplitudes around the mean value in the first few seconds, while in case of an open by-pass line the amplitudes attenuated faster and the pressure drops slightly. It is concluded that the closed-by-pass line scenario gives a slightly higher maximum dynamic forces and pressure amplitudes and slower attenuation of disturbance. The results for third scenario with the simultaneous closure of three stop valves in the RA 01, RA 02, and RA 03 sections and delayed closure of the valve in the RA 04 section are shown in figs. 10-17. Stop valves close in the RA 01, RA 02, and RA 03 sections in 0.15 seconds. The velocity change in front of the stop valve in these lines is practically the same and it is shown in fig. 10. The change of velocity in front of the stop valve in the RA 04 section, whose closure is delayed by 0.5 seconds, is shown in fig. 11. The velocity ahead of the delayed valve increases

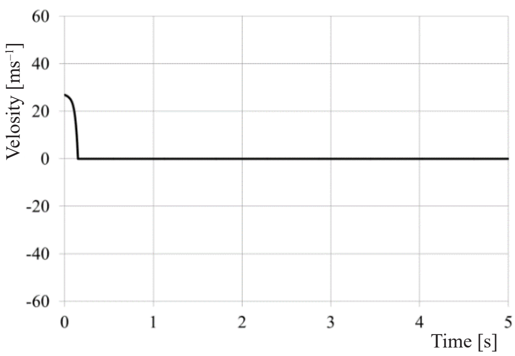

Figure 10. Steam velocity in the sections RA 01, RA 02, and RA 03 in front of the stop valves that are closed in 0.15 seconds, third scenario

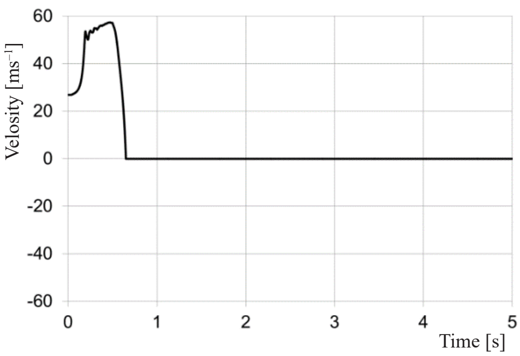

Figure 11. Steam velocity in the section RA 04 in front of the stop valve that is closed with the delay of 0.5 seconds, third scenario

from approximately 28 m/s to 58 m/s in the period from 0 s to 0.65 seconds due to the previous closure of other stop valves and the increased steam pressure. The dynamic forces exerted by the stop valves simultaneously close from 0 to 0.15 seconds, have practically the same character of periodic change and the same amplitude. These forces are presented in fig. 12 by the results obtained for the RA 03 section in front of the stop valve. The maximum amplitude of dynamic force is reached when the stop valve is closed at 0.15 seconds. Afterwards the dynamic force is attenuated within the short period and its amplitude is increased again after 0.65 seconds due to the stop valve closure in the RA 04 section. The dynamic force in the RA 04 section in front of the stop valve, whose closing is delayed by 0.5 seconds, is shown in fig. 13. As shown, the amplitude of approximately –10 kN occurs after 0.15 seconds due to the closure of the other three stop valves at 0.15 seconds. The negative sign of the force indicates that it acts in the opposite

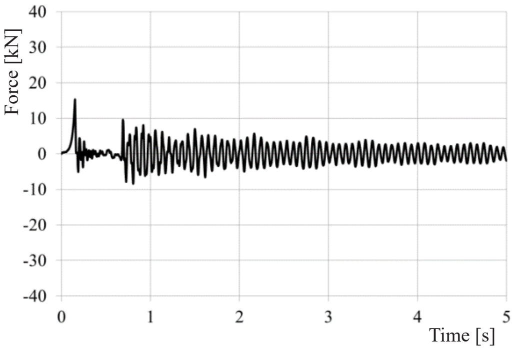

Figure 12. Dynamic force F_{EF} in the RA 03 section in front of the stop valve, in case with simultaneous closure of the valves in the RA 01, RA 02 and RA 03 sections and delayed closure of the valve in the RA04 section

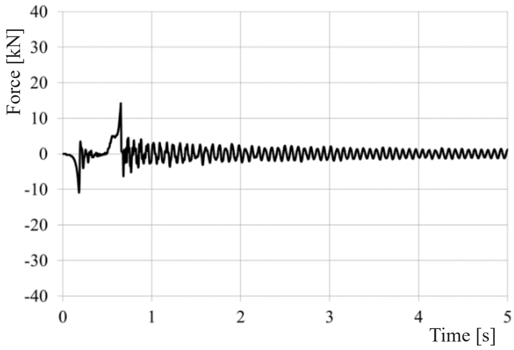

Figure 13. Dynamic force F_{GH} in the RA 04 section in front of the stop valve, in case with simultaneous closure of the valves in the RA 01, RA 02 and RA 03 sections and delayed closure of the valve in the RA04 section

direction to the steam flow direction before the valve closure. The second higher force impulse occurs after the valve is closed in the RA04 line at 0.65 seconds. The amplitude of the dynamic force in the RA 04 section at the closure of the stop valve is approximately the same as the amplitudes of the forces in the segments in front of other three stop valves that are closed 0.5 seconds earlier, as shown in figs. 12 and 13. The pressure changes in front of the stop valves in the segments RA 03 and RA 04 are shown in figs. 14 and 15. The results show practically the same periods and amplitudes of pressure change in front of both stop valves. Similar results of pressure change are obtained in front of the stop valves in the other two segments RA 01 and RA 02. The first pressure rise slightly above 190 bar occurs after the simultaneous closure of three valves, while the second pressure rise to approximately 195 bar occurs after the delayed closure of the fourth valve. Characteristic changes of the fluid dynamic force and pressure in sections along the pipeline are shown by the example of these parameters in the segment A-B at the RA 20 section in figs. 16 and 17. The comparison of the results in figs. 6 and 16 shows that the amplitude of the first maximum amplitude is substantially reduced from 37 kN in case with the simultaneous closure of all stop valves to 20 kN in case with the delayed closure of one stop valve. Pressure changes in case with delayed closure of one valve also show lower amplitudes compared to the case with the simultaneous closure of all valves, as shown by the comparison of figs. 9 and 17.

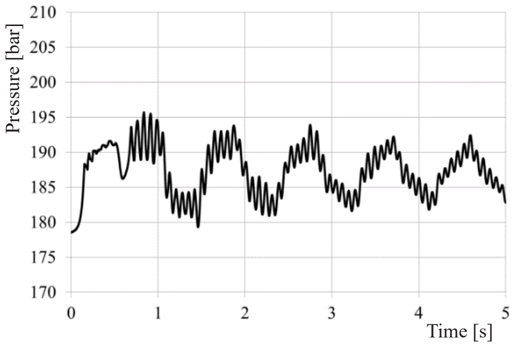

Figure 14. Steam pressure in front of the stop valve in the RA 03 section, in case with simultaneous closure of the valves in the RA 01, RA 02, and RA 03 sections and delayed closure of the valve in the RA04 section

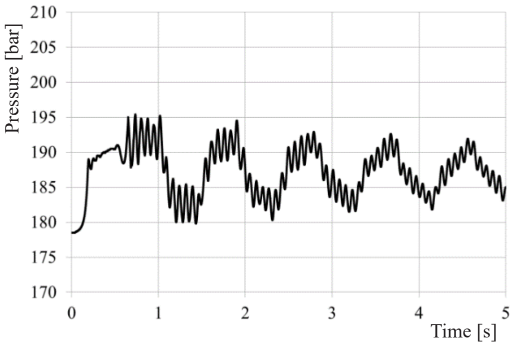

Figure 15. Steam pressure in front of the stop valve in the RA 04 section, in case with simultaneous closure of the valves in the RA 01, RA 02, and RA 03 sections and delayed closure of the valve in the RA04 section

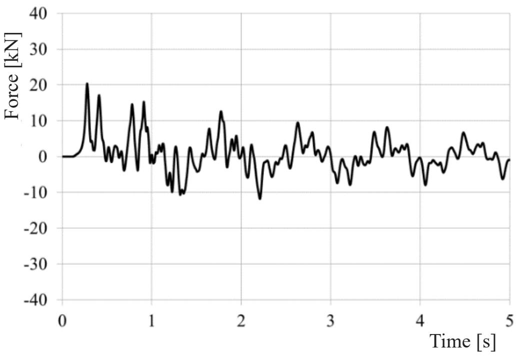

Figure 16. Dynamic force F_{AB} in the RA 20 section, in case with simultaneous closure of the valves in the RA 01, RA 02, and RA 03 sections and delayed closure of the valve in the RA 04 section

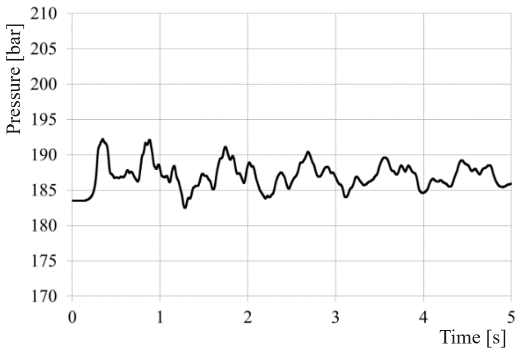

Figure 17. Steam pressure at the half length of the A-B part of the RA 20 section, in case with simultaneous closure of the valves in the RA 01, RA 02, and RA 03 sections and delayed closure of the valve in the RA 04 section

Conclusions

The numerical simulations and analysis of transient conditions in the main steam pipeline in 350 MWe coal-fired thermal power plant were conducted with the in-house code based on the method of characteristics. Transient conditions are caused by the closure of the stop valves in front of the HPT with and without opening of the steam by-pass line around the turbine. The presented results of simulations show fluid dynamic forces and pressure waves propagations. The major findings are as follows.

- Dynamic forces acting on the structure of the main steam pipeline after the stop valves closure in front of the HPT are maximal during the first pressure and fluid dynamic force peak that occur within one second after the stop valve closure.
- The maximum dynamic forces in the main steam pipeline during the first second after the turbine trip are practically the same in cases with and without the steam by-pass line opening.
- After approximately one second from the stop valves closure, dynamic forces along the main steam pipeline are damped more intensively in case with the open steam by-pass line than in case with the closed by-pass line.

- The delayed closure of one of the four stop valves leads to the increase of amplitudes of the fluid dynamic forces and pressure in the turbine steam admission line segments in front of the stop valves in comparison to the case with the simultaneous closure of all four stop valves.
- Contrary to the previous finding, the delayed closure of one of the four stop valves leads to the decrease of amplitudes of the fluid dynamic forces and pressure in segments along the pipeline, from the boiler exit headers to the main collector in front of the turbine steam admission lines.

Acknowledgment

The present research was supported by the Ministry of Education, Science and Technological Development of the Republic of Serbia (Grant 174014).

References

[1] Lahey, R. T., Moody, F. J., *The Thermal-Hydraulics of a Boiling Water Nuclear Reactors*, ANS Monograph, La Grange Park, Ill., USA, 1984, pp. 483-487
[2] Sun, W. S., Crim, G. C., Stress Analysis of Piping Systems, in: *Piping Handbook*, (Ed. M. L. Nayyar,), McGraw-Hill, Inc., New York, USA, 6th ed., 1992, pp. B.153-B.154
[3] Neises, G. J., Garrett, T. J., Steam Line Break Analysis Comparison to the Wolf Creek Updated Safety Analysis Report, *Nuclear Technology*, *93* (1991), 1, pp. 22-35
[4] McGeorge, R., Swec, L. F., The Steamhammer Problem: Dynamic Loading of Critical Reactor Piping Systems, *Nuclear Engineering and Design, 32* (1975), 1, pp. 121-128
[5] Stevanovic, V., *et al.*, Simulation and Analysis of a Main Steam Line Transient with Isolation Valves Closure and Subsequent Pipe Break, *International Journal of Numerical Methods for Heat & Fluid Flow, 4* (1994), 5, pp. 387-398
[6] Bayoumy, A. H., Papadopoulos, A., Time History Steam Hammer Analysis for Critical Hot Lines in Thermal Power Plants, *Proceedings,* ASME 2014 International Mechanical Engineering Congress and Exposition IMECE2014, Montreal, Canada, 2014, Nov., 14-20, IMCE2014-38076
[7] Wulff, W., Computational Methods for Multiphase flow, *Proceedings*, 2nd International Workshop on Two-Phase Flow Fundamentals, Rensselaer Polytechnic Institute, Troy, New York, USA, 1987, pp. 38-42
[8] Stoop, P. M., *et al.,* CHARME-01, a Thermo-Hydraulic Code for the Calculation of Fast Transients Inside Piping Systems, *Proceedings,* 8th International Conference on Structural Mechanics in Reactor Technology, Brussels, Belgium, 1985
[9] Choi, D. K., PIPES – a Computer Code for Analysis of Dynamic Hydraulic Response in Plant Piping Systems, Report No. CE NPSD-238, Combustion Engineering, Inc, Windsor, Canada, 1983
[10] ***, PIPENET VISION Transient Module User and Reference Manual Software Revision 1.5, Sunrise, 2010
[11] Milivojevic, S., *et al.,* Condensation Induced Water Hammer: Numerical Prediction, *Journal of Fluids and Structures*, *50* (2014), Oct., pp. 416-436
[12] Ivljanin, B., *et al*., Water Hammer with Non-Equilibrium Gas Release, *International Journal of Pressure Vessels and Piping*, *165* (2018), Aug., pp. 229-240
[13] Alghlam, A. S. M., *et al*., Numerical Simulation of Natural Gas Pipeline Transients, *Journal of Energy Resources Technology*, *Transactions of the ASME, 141* (2019), 10, 102002

Paper submitted: September 15, 2019
Paper revised: October 3, 2019
Paper accepted: October 10, 2019